JACS
JOURNAL OF THE AMERICAN CHEMICAL SOCIETY

Article

pubs.acs.org/JACS

Conformational Dynamics and Stability of HP35 Studied with 2D IR Vibrational Echoes

Jean K. Chung, Megan C. Thielges,[#] and Michael D. Fayer*

Department of Chemistry, Stanford University, Stanford, California 94305, United States

Supporting Information

ABSTRACT: Two-dimensional infrared (2D IR) vibrational echo spectroscopy was used to measure the fast dynamics of two variants of chicken villin headpiece 35 (HP35). The CN of cyanophenylalanine residues inserted in the hydrophobic core were used as a vibrational probe. Experiments were performed on both singly (HP35-P) and doubly CN-labeled peptide (HP35-P_2) within the wild-type sequence, as well as on HP-35 containing a singly labeled cyanophenylalanine and two norleucine mutations (HP35-P NleNle). There is a remarkable similarity between the dynamics measured in singly and doubly CN-labeled HP35, demonstrating that the presence of an additional CN vibrational probe does not significantly alter the dynamics of the small peptide. The substitution of two lysine residues by norleucines markedly improves the stability of HP35 by replacing charged with nonpolar residues, stabilizing the hydrophobic core. The results of the 2D IR experiments reveal that the dynamics of HP35-P are significantly faster than those of HP35-P NleNle. These observations suggest that the slower structural fluctuations in the hydrophobic core, indicating a more tightly structured core, may be an important contributing factor to HP35-P NleNle's increased stability.

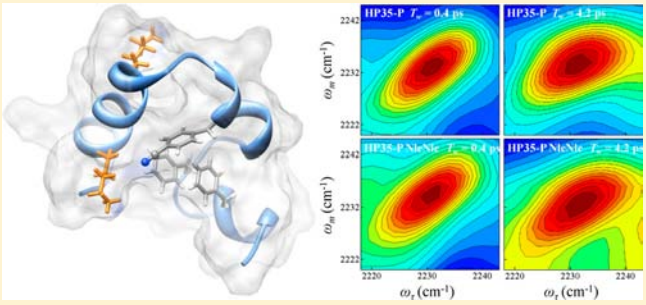

1. INTRODUCTION

One of the most difficult challenges in current biophysics is to accurately characterize the dynamics of proteins on fast time scales pertinent to their structure, stability, and function. Many endeavors in computational and experimental research groups have been geared toward this goal using a variety of methods.[1−3] Two-dimensional infrared (2D IR) vibrational echo spectroscopy is one such technique that possesses a unique ability to measure dynamics of proteins on the picosecond time scale under thermal equilibrium conditions.[4] Although it is generally believed that flexibility and dynamics play important roles in protein stability,[5−7] no direct measurement has been made to establish their relationship on a time scale of picoseconds. In this work, 2D IR vibrational echo spectroscopy was used to examine the relationship between the stability and ultrafast dynamics of the chicken villin headpiece 35 (HP35) using as vibrational probes CN groups inserted by substitution of phenylalanine residues with cyanophenylalanine.

HP35 is a small subdomain of the F-actin-binding protein villin that serves the biophysical research community as a bridge between computational and experimental studies.[8−11] Even though it is a relatively small peptide consisting of only 35 amino acids, HP35 has many characteristics associated with larger proteins. For example, it folds autonomously, has a hydrophobic core that stabilizes its tertiary structure, and has substantial structural resistance to various point mutations.[12,13] Furthermore, it is one of the fastest-folding peptides known, which makes it an attractive target for atomistic molecular dynamics simulations[14,15] and corroborating experimental methods, including FRET,[16] fluorescence,[12] mid-IR T-jump[17] spectroscopy, and triplet−triplet energy transfer.[18,19] Experimental examination of HP35 using ultrafast 2D IR spectroscopy is a more recent development, accelerated in part due to the realization that nitrile (CN) groups can be easily attached to the peptide to introduce a site-specific molecular oscillator to act as a vibrational dynamics label (VDL).[20−22]

In 2D IR studies of proteins, a good VDL would be sensitive to global structural changes of the proteins, while its perturbation on the structure and function would be minimal. The CN group has been actively pursued as a candidate for a VDL in biological systems owing to minimal perturbation, sensitivity to local electric field, and IR absorption in a relatively uncongested region of the mid-IR spectrum.[21,23] Research that has utilized CN as the VDL include linear vibrational spectroscopy[24] and 2D IR spectroscopy.[21,25,26] HP35 has been shown to be particularly amenable to the incorporation of a CN VDL because cyanophenylalanine may be introduced during standard solid-state synthesis of the peptide. In this work, HP35 variants with one (HP35-P) and two (HP35-P_2) cyanophenylalanines in the hydrophobic core were studied. It was found that, within experimental error, the dynamics of the two peptides measured by 2D IR experiments are the same. This result indicates that the substitution of phenylalanine with cyanophenylalanine is a very mild perturbation of the system. In addition, the CN VDL was used to measure the ultrafast

Received: March 28, 2012
Published: July 5, 2012

   dx.doi.org/10.1021/ja303017d | J. Am. Chem. Soc. 2012, 134, 12118−12124

dynamics of HP35 and its fast-folding mutant, HP35 NleNle, to investigate the relationship between dynamics and stability.

2. EXPERIMENTAL PROCEDURES

2.1. Sample Preparations. The peptides used in this study were prepared via solid-state peptide synthesis (Stanford Protein and Nucleic Acid Facility), with incorporation of *p*-cyano-L-phenylalanine (F_{CN}, Peptech) at residue Phe58 or at both residues Phe58 and Phe47. Figure 1 shows a structural representation of HP35-P from MD simulations with a single CN label on Phe58. The peptides sequences are $L_{42}SDEDFKAVFGMTRSAF_{CN}ANLPLWKQQHLKKEKGLF_{67}$ for HP35-P and $L_{42}SDEDFKAVFGMTRSAF_{CN}ANLLWnLQQHL$-$nLKEKGLF_{67}$ for HP35-P NleNle (nL represents norleucine). The peptides were purified by HPLC, and their purity was checked by ESI mass spectrometry. For the IR experiments, the peptides were dissolved in 50 mM sodium acetate buffer (pH 4.0) at a concentration of approximately 7 mM and sandwiched between two IR-transparent calcium fluoride windows with 25 μm Teflon spacers. This resulted in a CN stretching absorbance of 5 mOD at 2235 cm^{-1}. For CD experiments, the peptide concentration was 50 μM dissolved in the same solvent and in a 1 mm path length quartz cell.

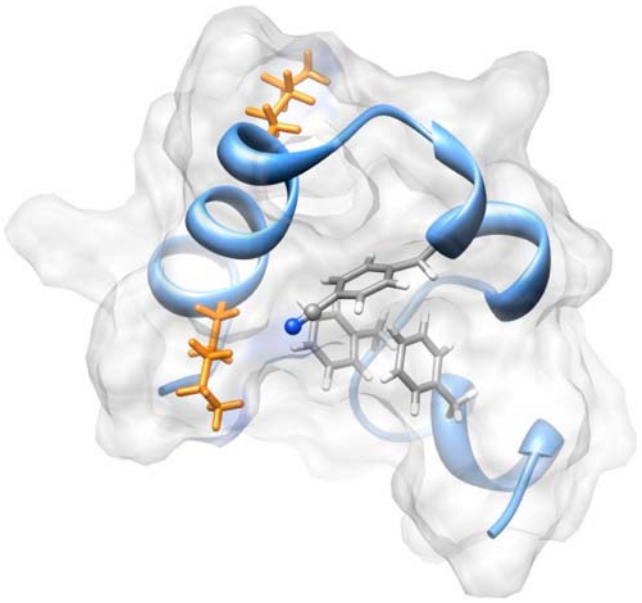

Figure 1. Structural representation of HP35-P. Phe58 has a CN functional group that serves as the vibrational probe. Two other phenylalanine residues participating in the aromatic stacking in the hydrophobic core are shown. Lys65 and Lys70 are highlighted in orange.

All of the experiments, time independent and time dependent, were conducted at 24 °C.

2.2. FT-IR and CD Spectroscopy. Absorption spectra were obtained with a Nicolet 6700 FT-IR spectrometer (Thermo Scientific) with 1 cm^{-1} resolution. The spectra of solvents were also collected for background subtraction, after which baselines were corrected by cubic spline. Circular dichroism (CD) spectra were measured in the far-UV region (200−250 nm, Jasco J810) at 1 nm resolution. The unfolding of the peptide was monitored at 222 nm.

2.3. 2D IR Vibrational Echo Spectroscopy. Detailed descriptions of the experimental methods[27] and conditions[21] for 2D IR vibrational echo experiments are provided elsewhere. In the experiments, 160 fs pulses at 1 kHz repetition rate with the transform-limited Gaussian spectrum (fwhm 90 cm^{-1}) centered at the CN absorption frequency, 2235 cm^{-1}, were used. Three focused excitation pulses, each about 1.2 μJ in energy, are crossed in the sample. The time between pulses 1 and 2 is called τ, and the time between pulses 2 and 3 is called T_w. The time-ordered interactions of the three pulses with the CN vibrational oscillators give rise to a fourth pulse, the vibrational echo, which emerges from the sample in a unique direction. The vibrational echo pulse is overlapped with another pulse, the local oscillator (LO), which is fixed in time. As τ is scanned, the echo pulse moves in time across the fixed LO pulse. Interference between the vibrational echo pulse and the LO produces a temporal interferogram which provides phase information necessary for Fourier transformation. The combined vibrational echo and LO wave packet is frequency-resolved in a monochromator used as a spectrograph. A 32-pixel HgCdTe array detector records the spectrum. Taking the spectrum provides one of the two Fourier transforms necessary to obtain the 2D IR spectrum. It yields the vertical ω_m axis of the 2D IR spectrum. Scanning the time between pulses 1 and 2 produces a temporal interferogram at each of the ω_m frequencies. Numerical Fourier transformation of these interferograms yields the horizontal ω_τ axis of the 2D IR spectrum. For a fixed T_w, τ is scanned, and a 2D IR spectrum is obtained. Then T_w is changed, and another spectrum is obtained. The changes in the 2D band shapes with T_w provide information on the time dependence of the peptide's structural fluctuation.

2D IR experiments measure the time evolution of the CN vibrational stretching frequency within the inhomogeneous distribution of vibrational frequencies reflected in the CN absorption spectrum. The theory and interpretation of 2D IR experiments have been described previously.[4,27] For each sample, 2D IR spectra are obtained as a function of waiting time, T_w. During T_w, the peptide structure undergoes conformational fluctuations, which cause the CN frequencies to evolve within the distribution of frequencies that comprise the inhomogeneous absorption spectrum. The evolution in frequencies of the CN vibrational oscillators is called spectral diffusion. The time dependence of the spectral diffusion, which is caused by the structural evolution of the peptide, is calculated from the time-dependent shape of the 2D IR vibrational echo spectra. The faster the peptide samples different conformations, the faster the 2D line shape changes. A robust method for calculating the spectral diffusion from the 2D IR spectra using the center line slope (CLS) formalism has been reported.[28,29] The CLS is closely related to the frequency−frequency correlation function (FFCF). The spectral diffusion is described by a FFCF, which is the connection between the experimental observables and the underlying dynamics of the peptide.[28,29] The CLS is essentially the normalized FFCF with the offset from 1 at $T_w = 0$ determined by the homogeneous component of the dynamics (see below). Combining the CLS data and the IR absorption line shape permits the determination of the FFCF.[28,29] The CLS also provides a convenient method of displaying and comparing the time-dependent structural dynamics of the peptides.

The FFCF is modeled with a multiexponential function,

$$C(t) = \sum_{i=1}^{n} \Delta_i^2 \, e^{-t/\tau_i} + \Delta_s \tag{1}$$

where Δ_i (rad/s) is the amplitude of the ith component of the frequency fluctuation and τ_i is the associated time constant. The static term Δ_s represents the contribution to the CN frequency distribution that arises from the peptide structural fluctuations that are so slow that they fall outside the experimental time window, which is determined by the vibrational lifetime of the CN stretching mode. If $\Delta\tau < 1$, this component of the frequency fluctuations is motionally narrowed (homogeneous broadening), and Δ and τ cannot be determined separately. The motionally narrowed homogeneous contribution to the absorption spectrum has a pure dephasing line width given by $\Gamma^* = \Delta^2\tau = 1/\pi T_2^*$, where T_2^* is the pure dephasing time. The homogeneous line width is dominated by pure dephasing, but the observed homogeneous dephasing time, T_2, also has contributions from the vibrational lifetime,

$$\frac{1}{T_2} = \frac{1}{T_2^*} + \frac{1}{2T_1} \tag{2}$$

dx.doi.org/10.1021/ja303017d | J. Am. Chem. Soc. 2012, 134, 12118−12124

where T_2^* and T_1 are the pure dephasing time and the vibrational lifetime, respectively. The total homogeneous line width is then $\Gamma = 1/\pi T_2$. The vibrational lifetime was measured with an IR pump−probe experiment, T_1 = 4.5 ps. For the experiments discussed below, the homogeneous component, a single exponential decay term, and the static term are sufficient to fit the data.

3. RESULTS AND DISCUSSIONS

3.1. Influence of Nitrile Labeling on Peptide Dynamics. An important question is how much does the labeling with CN influence the properties, particularly the dynamics, of the HP35 peptide? The CN of an artificial amino acid, cyanophenylalanine, was used as the VDL. HP35-P has been studied by Glasscock et al. using FRET[16] and by Urbanek et al. with 2D IR experiments.[26] The dynamics of guanidinium-unfolded HP35-P_2, the wild-type HP35 sequence with two CN labels (Phe47Phe_{CN}/Phe58Phe_{CN}), have been investigated using 2D IR vibrational echoes as well.[21] In all these works it was suggested that the overall structure of the peptides is not significantly altered as the result of the incorporation of CN labels in the hydrophobic core.

We cannot compare HP35 to HP35-P by infrared methods because HP35 does not have a VDL. However, we can compare HP35 with a single cyanophenylalanine, HP35-P, and one with two cyanophenylalanines, HP35-P_2. (In a previous publication, HP35-P_2 was called HP35-$(CN)_2$.[21]) In HP35-P_2, there are two CN labels, one at Phe47 and another at Phe58. Comparison of HP35-P and HP35-P_2 can provide information on whether the insertion of the CN groups affects the peptide's properties.

Figure 2 shows the FT-IR absorption spectra of the CN stretch of HP35-P and HP35-P_2. The inset shows the spectrum

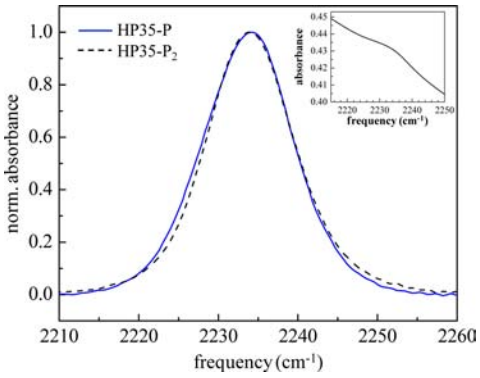

Figure 2. FT-IR spectra of the CN stretching mode of HP35-P (blue) and HP35-P_2 (black). The inset shows the spectrum prior to the background subtraction of a large water absorption band. Within experimental error the two spectra are identical.

of HP35-P_2 before background subtraction. The nitrile absorption is a small feature on top of a very large water sloping background. To obtain the spectra shown in the main part of Figure 2 requires subtraction of the large background, which can introduce small errors in the line shape. Therefore, within experimental error, the two absorption spectra are the same. In addition, 1D H^1NMR downfield chemical shifts and the results of 2D NOESY, COSY, and HSQC are consistent with the picture that the environments experienced by the two CN groups are virtually identical. (The NMR results are presented in detail in the Supporting Information.) The examination of the peptide structure (PDB 1YRF) supports the same conclusion as the NMR studies, as Phe47 and Phe58 are next to each other to form tight aromatic stacking, and the CN groups on each phenyl rings would occupy similar positions in the hydrophobic core.

Figure 3 shows the CLS data for HP35-P (blue circles) and for HP35-P_2 (black circles). The CLS for HP35-P_2 was

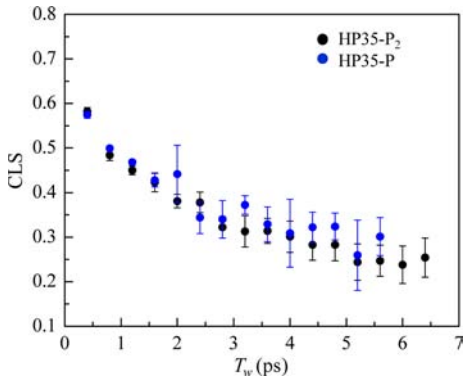

Figure 3. CLS data for the CN stretching mode of HP35-P (blue) and HP35-P_2 (black). Within experimental error the data are identical, which demonstrates that the addition of a second CN vibrational dynamics label (HP35-P_2) does not change the structural fluctuations of the peptide.

analyzed in the same manner as HP35-P although there are two VDLs contributing to the signal. CLS analysis of a 2D spectrum with two VDLs has been treated in detail theoretically.[30] For the case when the two absorption spectra are the same, the CLS for two VDLs is the average of their CLS. If adding a second cyanophenylalanine changed the peptides dynamics, then the observed CLS would reflect the change. As can be seen from the figure, within experimental error, the two sets of data are identical. Therefore, adding a second cyanophenylalanine does not change either the absorption spectrum or the structural dynamics. This is in contrast to the substitution of two lysine residues by norleucines, which does have a substantial influence on the structural dynamics as well as a change in the CN absorption peak position (see below). Going from one CN VDL to two CN VDLs has little or no effect on the structure as indicated by the spectra in Figure 2 and on the dynamics, as shown by the CLS data in Figure 3. These results suggest that going from no CN VDL to one CN VDL will cause only small perturbations of the peptide's structure and dynamics. The comparison of HP35-P and HP35-P_2 is the first time that such an assessment has been made. These results are important because they suggest that in larger proteins, CN VDLs will produce only small changes to the protein's structure and dynamics.

3.2. Influence of Mutation on Peptide Dynamics. Two HP35 variants with a single CN label were compared. They are wild-type HP35 with the CN label at Phe58 (HP35-P), and the double norleucine mutant (Lys65Nle/Lys70Nle) with the CN label at the same position (HP35-P NleNle). HP35 NleNle is a product of efforts to engineer a fast folding peptide.[12,31] Clues for mutating Lys65 and Lys70 to Nle came from high-resolution X-ray crystal structures, which showed charged lysine groups buried inside the hydrophobic core of HP35. The peptide with a double norleucine mutation, Lys65Nle/Lys70Nle, was shown to fold 2.6 times faster with a folding time of 0.7 μs and to be more stable by 4 kJ/mol compared to the wild type.[31] The increased stability and folding rate are thought to originate from the combined effects of reduced

dx.doi.org/10.1021/ja303017d | J. Am. Chem. Soc. 2012, 134, 12118−12124

unfavorable electrostatic clashing inside the hydrophobic core by the removal of the charged lysine residues and the destabilization of the unfolded state by introducing water-insoluble residues in the peptide sequence.[31] While both factors likely contribute to the stability of HP35 NleNle, it is difficult to separate one effect from another to determine the basis of stability. Measuring the structural dynamics of HP35-P and HP35-P NleNle can provide insights into the origin of stability. The CN VDL is sensitive to local as well as global structure and structural fluctuations as discussed below.[32] In both peptides, the VDL is in the interior hydrophobic core.

The stability difference between wild-type HP35 and HP35 NleNle was measured using temperature-dependent CD at pH 4.8.[11,31] The current experiments were conducted at pH 4 to give sufficient solubility for the 2D IR experiments and the two types of peptides each have a CN label. Given the pK_a values of the two glutamic acids and the two aspartic acids in the peptide, the lower pH has a major effect on the protonation of these acidic amino acids. To see whether at pH 4 HP35-P NleNle has a similar increase in stability compared to HP35-P as previously observed for the unlabeled peptides, temperature-dependent CD experiments were obtained and displayed in Figure 4 for

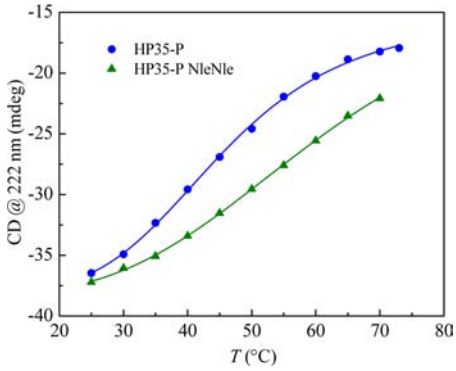

Figure 4. Unfolding of HP35-P (blue circles) and HP35-P NleNle (green triangles) measured with CD signal at 222 nm. The results show the increased stability of HP35-P NleNle relative to HP35-P, which has been reported previously for NNHP35 and HP35.

HP35-P (blue curve) and HP35-P NleNle (green curve). The CD signal was monitored at 222 nm to follow changes in the alpha helical content, and two-state model fits yielded T_m values of ~45 and ~62 °C for HP35-P and NleNleHP35-P, respectively. Both samples show apparent sigmoidal transitions, with the HP35-P NleNle being significantly more stable than HP35-P. The difference of ~17 °C between the two curves shown in Figure 4 is almost the same as those obtained previously for HP35 and HP35-P NleNle at pH 4.8, ~20 °C.[11,31] Therefore, the increase in stability of HP35 NleNle compared to HP35 is preserved for HP35-P NleNle compared to HP35-P at pH 4.

Figure 5 displays normalized linear absorption spectra of the CN stretch of HP35-P (blue) and HP35-P NleNle (green). Each curve is the average of measurements on three samples. The center frequencies of the CN absorptions are 2233.8 ± 0.2 and 2233.0 ± 0.2 cm^{-1} for the wild type and the norleucine mutant, respectively. Both bands have the full width at half-maximum (fwhm) of 13.5 ± 0.2 cm^{-1}. Red shifts in the frequencies of aromatic CN absorptions are often associated with the CN being in more hydrophobic environments.[22,33] Then, the small red shift of HP35-P NleNle may be due to the

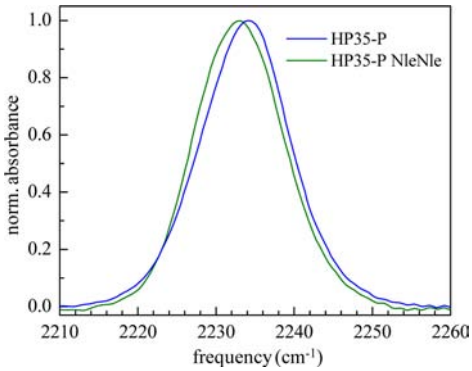

Figure 5. FT-IR spectra of the CN stretching mode in HP35-P (blue) and HP35-P NleNle (green). The center frequencies are 2233.8 ± 0.2 and 2233.8 ± 0.2 cm^{-1} for HP35-P and HP35-P NleNle, respectively. The full width at half-maximum (fwhm) is 13.5 ± 0.2 cm^{-1} for both peptides.

double norleucine mutation, which renders the interior of the hydrophobic core even more hydrophobic.

2D IR vibrational echo spectra of HP35-P (top panels) and HP35-P NleNle (bottom panels) are shown in Figure 6. Only

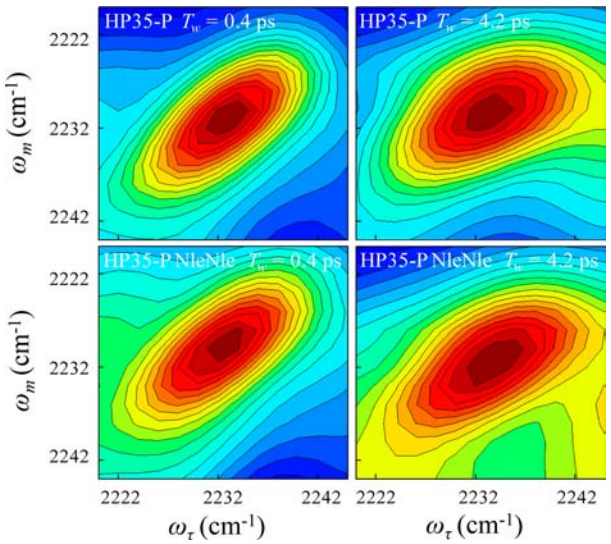

Figure 6. 2D IR vibrational echo spectra of the CN in HP35-P (top row) and HP35-P NleNle (bottom row) at T_w = 0.4 ps (left panels) and T_w = 4.2 ps (right panels).

the portion of the spectrum arising from the vibrational ground state and first excited state are shown. At short T_w (0.4 ps) the bands are more elongated than at longer T_w (4 ps). The change in shape is the signature of spectral diffusion caused by structural fluctuations of the peptides. Note that the change in shape of the HP35-P spectrum (top panels) is greater than the change in the HP35-P NleNle spectrum (bottom panels). This difference indicates that structural dynamics are slower in HP35-P NleNle than in HP35-P.

Figure 7 shows the CLS data from the 2D IR experiments for HP35-P (blue) and HP35-P NleNle (green). Each point in the CLS plot represents the average of three experimental repetitions performed on three separately prepared samples. The error bars on the points are the equivalent of those shown for the blue circles in Figure 3. The CLS curves do not decay to zero because data collection is limited by the vibrational lifetime

dx.doi.org/10.1021/ja303017d | J. Am. Chem. Soc. 2012, 134, 12118−12124

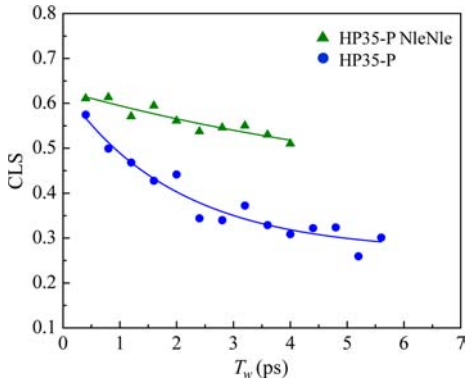

Figure 7. CLS decay data for HP35-P (blue circles) and HP35-P NleNle (green triangles). The data show clearly that the structural dynamics of the mutant HP35-P NleNle are significantly slower than those of HP35-P.

of the CN stretch (4.5 ps). It is evident from Figure 7 that the dynamics of HP35-P NleNle accessed in the time window of the experiment are substantially slower than those of HP35-P. The FFCF parameters are given in Table 1. The homogeneous line width, Γ^*, and the homogeneous pure dephasing time, T_2^*, are identical within experimental error for HP35-P NleNle and HP35-P. The major difference in the dynamics of the two peptides is the decay time, τ_1, which is associated with the spectral diffusion that occurs within the experimental time window. With the double norleucine mutation, the spectral diffusion decay time is 7 ps compared to the 2 ps for HP35-P. Thus, the dynamics at short time are substantially slower for the mutant. In addition, there are small differences in the amplitude factors, Δ_1 and Δ_s. For HP35-P NleNle, Δ_s is somewhat bigger and Δ_1 is somewhat smaller than the corresponding values for HP35-P. Because the homogeneous linewidths and the absorption line widths (see Figure 5) are the same, an increase in Δ_s and a decrease in Δ_1 for HP35-P NleNle compared to HP35-P indicate a shift of some of the structural dynamics to longer times. Therefore, the spectral diffusion time associated with fast structural fluctuation for HP35-P NleNle is slower, and a larger fraction of the structural dynamics is shifted to the slow time scale outside of the experimental window compared to the corresponding components found for HP35-P. The result is an overall shift of the dynamics, those that are observed and those that are too slow to observe to longer times.

The spectral diffusion shown by the CLS curves in Figure 7 reflect sampling of the conformational structures that give rise to the IR absorption spectra. If the experiments could be conducted to much longer times, the CLS curves would decay to zero because on some time scale all conformations will be sampled. Here, only a portion of all possible structures are sampled in the experimental time window. For HP35-P, approximately 70% of the states that give rise to the absorption line are sampled, while for HP35-P NleNle approximately 50% are sampled. Although the time window is short, in both cases a significant fraction of the structural configurations that give rise to the absorption spectrum are sampled.

To put the differences reflected by the curves in Figure 7 into perspective, it is useful to discuss 2D IR vibrational echo experiments and simulations of other proteins. Detailed 2D IR studies of myoglobin with CO attached at the active site (Mb-CO) and several Mb-CO mutants have been performed[34] and simulations have been used to explicate the data. In these experiments, CO is the VDL. In myoglobin and myoglobin mutants such as L29I-CO and a double mutation, T67R/S92D-CO, there are two prominent bands in the in the IR absorption spectrum. Loring and co-workers have been quite successful in simulating the spectral diffusion of both Mb-CO and T67R/S92D-CO. The simulations show very good agreement with the vibrational echo experiments.[35] In the simulations, the CO is coupled to the fluctuating protein structure through Stark coupling. In the simulations, the electric field from the entire protein and solvent is determined along the CO bond. Then, the electric field-electric field correlation function is calculated. When this correlation function is multiplied by a Stark coupling constant, the result is the FFCF.

There are two facts from simulations that are important to the work presented here. First, for Mb-CO, the Stark coupling constant necessary to reproduce the spectroscopic data agrees with the experimental value.[34] Second, to determine the origin of the fluctuations that give rise to the experimental spectral diffusion described by the FFCF, the simulation of the protein was divided into concentric shells. It was found that there are contributions to the spectral diffusion from the entire protein. The CO VDL measures global fluctuations in addition to very local contributions.

Additional insight into the origin of the measured spectral diffusion comes from a study of the mutant H64V-CO. In this mutant, the distal histidine is replaced by a valine. Removing the distal histidine, which is in the heme pocket and has strong interactions with the CO, collapses the two IR spectral peaks into a single peak. The single peak is shifted substantially to higher frequency and its absorption spectrum is much narrower. In addition, the vibrational echo experiments reveal slower spectral diffusion. The conclusion is that a significant portion of the inhomogeneous line of Mb-CO comes directly from very local interactions with the distal histidine, and some of the fast structural fluctuations that give rise to the measured spectral diffusion come from motions of the distal histidine. However, in the absence of the distal histidine, there is still substantial inhomogeneous broadening and spectral diffusion, which arise from the non-local coupling of the protein motions to the CO.

Recently it has been shown that the same fluctuating electric field model applies to CN as a VDL. The protein, RNase-S was labeled with a CN, and 2D IR experiments were used to determine the spectral diffusion and the FFCF.[36] Detailed simulations came relatively close to reproducing the FFCF. The important aspect of RNase-S simulations is that the Stark coupling constant that related the electric field-electric field

Table 1. FFCF Parameters

sample	Γ^* (cm^{-1})	T_2^* (ps)	τ_1 (ps)	Δ_1 (cm^{-1})	Δ_s (cm^{-1})
HP35-P NleNle	3.8 ± 1.2	2.8 ± 0.8	6.9 ± 2.4	2.9 ± 0.3	3.5 ± 0.3
HP35-P	3.8 ± 0.7	2.8 ± 0.5	2.0 ± 0.5	3.4 ± 0.2	3.0 ± 0.2
$HP35\text{-}P_2$	3.8 ± 0.3	2.8 ± 0.25	2.2 ± 0.3	3.7 ± 0.1	2.7 ± 0.1

dx.doi.org/10.1021/ja303017d | J. Am. Chem. Soc. 2012, 134, 12118−12124

correlation function to the FFCF and the spectroscopic observables was again close to the value measured on an aromatic nitrile with static Stark spectroscopy. The Stark constant needed to get the best agreement with the RNase-S experiments was only ∼10% off from the measured value. Therefore, it is reasonable to take the Stark coupling mechanism to be appropriate for nitrile probes.

The results outlined briefly above can explain the results obtained in this study comparing HP35-P to HP35-P NleNle. In contrast to the major changes in the absorption spectrum in going from Mb-CO to H64V-CO, going from HP35-P to HP35-P NleNle produces no dramatic changes in the FT-IR absorption spectrum. There is a small shift, but of more importance, as the two line shapes are virtually identical. The lack of change of the line width indicates that there is no substantial change in local interaction with the CN in the mutant peptide. Therefore, like H64V-CO, which lacks the strong local contribution to the inhomogeneous line and dynamics, the inhomogeneous broadening and the dynamics of HP35-P to HP35-P NleNle have substantial global contributions. The fact that the inhomogeneous lines have the same widths suggests that the range of structures that give rise to the absorption line shape are very similar.

The 2D IR experiments show that the homogeneous line widths are the same within experimental error. As discussed above a greater fraction of the structural states of HP-35P are sampled on the very fast time scale compared to HP35-P NleNle, ∼70% vs 50%. Based on the discussion given immediately above, the states that are sampled involve global motions of the peptide, near and far, rather than only very local fluctuations. One possible explanation for the observed differences in dynamics is that the stability of HP35-P NleNle originates in part from better packing of the hydrophobic core, which in turn affects the dynamics of the entire peptide. The double mutant is more thermally stable than HP35-P as shown by the temperature-dependent CD curves, and it also folds faster as demonstrated by both simulations and experiments.[10,11] Now we see that the double mutant has significantly slower equilibrium structural fluctuations on the fast time scale accessed by the experiments and a larger percentage of configuration sampling is pushed out to longer time scales. The greater thermal stability is associated with a deeper free energy minimum for the folded double mutant.[3,37] The slowing of the structural fluctuations of the folded double mutant peptide indicates a rougher energy landscape with deeper local structural minima for those structures that are sampled fast. At least on the fast time scale, HP35-P might be thought of as having greater conformational flexibility than HP35-P NleNle. The inverse relationship between conformational flexibility and thermal stability has been previously studied using other experimental methods, such as NMR[5,38] and neutron scattering,[6,7] and hydrogen/deuterium exchange.[39,40]

4. CONCLUDING REMARKS

The influence of adding a CN as a vibrational label to HP35 using the artificial amino acid cyanophenylalanine was investigated. HP35-P with one cyanophenylalanine was compared to HP35-P_2 having two cyanophenylalanines. Both the absorption spectra and the dynamics measured by the 2D IR experiments were identical within experimental error. Therefore, the additional CN group causes at most a very small perturbation of the structure and the dynamics of HP35-P. These results suggest that CN used as a vibrational label should cause little perturbation of larger proteins.

In this work, the fast structural dynamics of HP35-P and its fast-folding mutant HP35-P NleNle were compared using 2D IR vibrational echo experiments on the CN stretch of cyanophenylalanine inside the peptides' hydrophobic cores. Vibrational absorption and CD spectroscopies were used to monitor changes to the structure and stability of the peptides. On the fast time scale investigated in the experiments, substantially slower dynamics were observed for HP35-P NleNle, which has two charged amino acids in the hydrophobic core replaced by nonpolar amino acids. The mutation produces a more stable peptide as evidenced by the temperature-dependent CD spectra for the CN-labeled peptides reported here, which is consistent with previous CD measurements for the unlabeled peptides.[11,31] The slowing of the fast structural fluctuations of the mutant indicates deeper wells separating the fast interconverting structures. While the limited time range of the 2D IR experiments prevents the observation of the interconversion among all structures, a non-negligible fraction of the conformations that give rise to the absorption line are observes, ∼70% for HP35-P and ∼50% for HP35-P NleNle. The results suggest that the increased stability of the mutant and its faster folding have a substantial contribution from changes in the structure of the folded peptide. The data presented on HP35-P and HP35-P NleNle are appropriate targets for MD simulations given the small size of the peptides and the short time scale of the measurements.

■ ASSOCIATED CONTENT

Supporting Information

Additional information on the NMR studies. This material is available free of charge via the Internet at http://pubs.acs.org.

■ AUTHOR INFORMATION

Corresponding Author

fayer@stanford.edu

Present Address

[#]Department of Chemistry, Indiana University, Bloomington, IN 47405

Notes

The authors declare no competing financial interest.

■ ACKNOWLEDGMENTS

We are grateful to Yeonju Kwak for assistance in CD data collection. We thank Kyle Beauchamp for providing the material for Figure 1, which came from MD simulations he performed. This work was supported by the National Institutes of Health (2-R01-GM061137-09).

■ REFERENCES

(1) Shaw, D. E.; Maragakis, P.; Lindorff-Larsen, K.; Piana, S.; Dror, R. O.; Eastwood, M. P.; Bank, J. A.; Jumper, J. M.; Salmon, J. K.; Shan, Y. B.; Wriggers, W. *Science* **2010**, *330*, 341−346.

(2) Hammes-Schiffer, S.; Benkovic, S. J. *Annu. Rev. Biochem.* **2006**, *75*, 519−541.

(3) Frauenfelder, H.; Sligar, S. G.; Wolynes, P. G. *Science* **1991**, *254*, 1598−1603.

(4) Finkelstein, I. J.; Zheng, J.; Ishikawa, H.; Kim, S.; Kwak, K.; Fayer, M. D. *Phys. Chem. Chem. Phys.* **2007**, *9*, 1533−1549.

(5) Stone, M. J. *Acc. Chem. Res.* **2001**, *34*, 379−388.

(6) Tsai, A. M.; Udovic, T. J.; Neumann, D. A. *Biophys. J.* **2001**, *81*, 2339−2343.

(7) Gabel, F.; Bicout, D.; Lehnert, U.; Tehei, M.; Weik, M.; Zaccai, G. *Q. Rev. Biophys.* **2002**, *35*, 327−367.
(8) Wang, M. H.; Tang, Y. F.; Sato, S. S.; Vugmeyster, L.; McKnight, C. J.; Raleigh, D. P. *J. Am. Chem. Soc.* **2003**, *125*, 6032−6033.
(9) McKnight, C. J.; Matsudaira, P. T.; Kim, P. S. *Nat. Struct. Biol.* **1997**, *4*, 180−184.
(10) Bowman, G. R.; Pande, V. S. *Proc. Natl. Acad. Sci. U.S.A.* **2010**, *107*, 10890−10895.
(11) Kubelka, J.; Henry, E. R.; Cellmer, T.; Hofrichter, J.; Eaton, W. A. *Proc. Natl. Acad. Sci. U.S.A.* **2008**, *105*, 18655−18662.
(12) Kubelka, J.; Eaton, W. A.; Hofrichter, J. *J. Mol. Biol.* **2003**, *329*, 625−630.
(13) Frank, B. S.; Vardar, D.; Buckley, D. A.; McKnight, C. J. *Protein Sci.* **2002**, *11*, 680−687.
(14) Zagrovic, B.; Pande, V. S. *J. Am. Chem. Soc.* **2006**, *128*, 11742−11743.
(15) Bowman, G. R.; Ensign, D. L.; Pande, V. S. *J. Chem. Theory Comput.* **2010**, *6*, 787−794.
(16) Glasscock, J. M.; Zhu, Y. J.; Chowdhury, P.; Tang, J.; Gai, F. *Biochemistry* **2008**, *47*, 11070−11076.
(17) Brewer, S. H.; Song, B. B.; Raleigh, D. P.; Dyer, R. B. *Biochemistry* **2007**, *46*, 3279−3285.
(18) Reiner, A. *J. Pept. Sci.* **2011**, *17*, 413−419.
(19) Reiner, A.; Henklein, P.; Kiefhaber, T. *Proc. Natl. Acad. Sci. U.S.A.* **2010**, *107*, 4955−4960.
(20) Getahun, Z.; Huang, C. Y.; Wang, T.; De León, B.; DeGrado, W. F.; Feng, G. *J. Am. Chem. Soc.* **2003**, *125*, 405−411.
(21) Chung, J. K.; Thielges, M. C.; Fayer, M. D. *Proc. Natl. Acad. Sci. U.S.A.* **2011**, *108*, 3578−3583.
(22) Waegele, M. M.; Culik, R. M.; Gai, F. *J. Phys. Chem. Lett.* **2011**, *2*, 2598−2609.
(23) Suydam, I. T.; Boxer, S. G. *Biochemistry* **2003**, *42*, 12050−12055.
(24) Fafarman, A. T.; Webb, L. J.; Chuang, J. I.; Boxer, S. G. *J. Am. Chem. Soc.* **2006**, *128*, 13356−13357.
(25) Fang, C.; Bauman, J. D.; Das, K.; Remorino, A.; Arnold, E.; Hochstrasser, R. M. *Proc. Natl. Acad. Sci. U.S.A.* **2008**, *105*, 1472−1477.
(26) Urbanek, D. C.; Vorobyev, D. Y.; Serrano, A. L.; Gai, F.; Hochstrasser, R. M. *J. Phys. Chem. Lett.* **2010**, *1*, 3311−3315.
(27) Park, S.; Kwak, K.; Fayer, M. D. *Laser Phys. Lett.* **2007**, *4*, 704−718.
(28) Kwak, K.; Park, S.; Finkelstein, I. J.; Fayer, M. D. *J. Chem. Phys.* **2007**, *127*, 124503.
(29) Kwak, K.; Rosenfeld, D. E.; Fayer, M. D. *J. Chem. Phys.* **2008**, *128*, 204505.
(30) Fenn, E. E.; Fayer, M. D. *J. Chem. Phys.* **2011**, *135*, 07450.
(31) Kubelka, J.; Chiu, T. K.; Davies, D. R.; Eaton, W. A.; Hofrichter, J. *J. Mol. Biol.* **2006**, *359*, 546−553.
(32) Merchant, K. A.; Thompson, D. E.; Xu, Q.-H.; Williams, R. B.; Loring, R. F.; Fayer, M. D. *Biophys. J.* **2002**, *82*, 3277−3288.
(33) Lee, H.; Choi, J. H.; Cho, M. *Phys. Chem. Chem. Phys.* **2010**, *12*, 12658−12669.
(34) Merchant, K. A.; Noid, W. G.; Akiyama, R.; Finkelstein, I.; Goun, A.; McClain, B. L.; Loring, R. F.; Fayer, M. D. *J. Am. Chem. Soc.* **2003**, *125*, 13804−13818.
(35) Bagchi, S.; Nebgen, B. T.; Loring, R. F.; Fayer, M. D. *J. Am. Chem. Soc.* **2010**, *132*, 18367−18376.
(36) Bagchi, S.; Boxer, S. G.; Fayer, M. D. *J. Phys. Chem. B* **2012**, *116*, 4034−4042.
(37) Onuchic, J. N.; LutheySchulten, Z.; Wolynes, P. G. *Annu. Rev. Phys. Chem.* **1997**, *48*, 545−600.
(38) Buck, M.; Boyd, J.; Redfield, C.; Mackenzie, D. A.; Jeenes, D. J.; Archer, D. B.; Dobson, C. M. *Biochemistry* **1995**, *34*, 4041−4055.
(39) Hernandez, G. J.; Jenney, F. E.; Adams, M. W. W.; LeMaster, D. M. *Proc. Natl. Acad. Sci. U.S.A.* **2000**, *97*, 3166−3170.
(40) Hiller, R. Z.; Zhou, Z. H.; Adams, M. W. W.; Englander, S. W. *Proc. Natl. Acad. Sci. U.S.A.* **1997**, *94*, 11329−11332.